**Science of Tsunami Hazards**
**Volume 43 Number 2 2025**
**ISSN 8755-683**

# Contents

**HYDRODYNAMIC ECHOES: AN INVESTIGATION OF SEICHE ACTIVITY FOLLOWING THE MARCH 28, 2025 MYANMAR EARTHQUAKE** ..... 1

*Aggeliki Barberopoulou[1, 2,*], George Malaperdas[3], Sarah Firth[2]* ..... 1

**TSUNAMIS IN ANTARCTICA, A STATISTICAL ANALYSIS** ..... 21

*R. Kh. Mazova, [1,*], N. A. Zhukov[1], E.F Denisov[1]* ..... 21

**SCIENCE OF TSUNAMI HAZARDS** is a **CERTIFIED OPEN ACCESS** Journal included in the prestigious international academic journal database DOAJ. **SCIENCE OF TSUNAMI HAZARDS** is also preserved, archived and disseminated by the National Library, The Hague, NETHERLANDS, the Library of Congress, Washington D.C., USA, the Electronic Library of Los Alamos, National Laboratory, New Mexico, USA, the EBSCO Publishing databases and ELSEVIER Publishing in Amsterdam.

**OBJECTIVE:** Tsunami Society International publishes this interdisciplinary journal to increase and disseminate knowledge about tsunamis and their hazards.

ISSN 8755-6839

SCIENCE OF TSUNAMI HAZARDS

The Journal of Tsunami Society International

Volume 43 Number 2 2025

# Hydrodynamic Echoes: An Investigation of Seiche Activity Following the March 28, 2025 Myanmar Earthquake

*Aggeliki Barberopoulou*[1, 2, *], *George Malaperdas*[3], *Sarah Firth*[2]

[1] *Hellenic Center for Marine Research, Anavyssos, Attiki Greece*

[2] *Tsunami Society International, Derry NH 03038 United States*

[3] *Department of History, Archaeology and Cultural Resources Management, University of the Peloponnese, Old Campus 24133, Kalamata, Greece*

* Aggeliki Barberopoulou, Email:a.barberopoulou@hcmr.gr

**Abstract**

This article presents a unique dataset of standing waves, also known as seiches, observed in swimming pools and other small bodies of water (ponds, lakes, fish tanks etc.) near the epicenter of the M7.7 Myanmar earthquake and in neighboring countries. While this phenomenon of seiching is not frequently documented on such a scale, these waves may provide valuable insights. Although this dataset is certainly not exhaustive due to its reliance on reported observations (versus available observations), these collected observations are crucial to better understand the initiation of seiches due to earthquake ground motions and their dependence on local geological and geomorphological characteristics. This study aims to contribute to the field by providing a unique collection of records linked to this seismic effect.

**Keywords:** Myanmar, seiches, 28 March 2025 Myanmar earthquake

## 1. Introduction

*Seiches* is a more sophisticated term used to describe standing waves generated in enclosed or semi-enclosed water basins due to a disturbance. The generating mechanism can vary, but the focus of this work is on seismic seiches—those caused by ground shaking due to an earthquake (e.g. Kvale, 1955; McGarr, 1965; McGarr and Vorhis, 1968; Barberopoulou et al. 2004, 2006; Rabinovich, 2009). Both distant and regional earthquakes have been associated with the generation of these waves, but local earthquakes can cause them as well (e.g. Kvale, 1950¥5;Canitano et al. 2017; Barberopoulou et al. 2023). Such waves have been observed as early as the 18$^{th}$ century (Forel, 1876; Wilson, 1972), but most of the available data remains limited in size (i.e., number of observations per event).

In general, reported observations of seiches are infrequent and lack spatial or temporal density, with very few exceptions (McGarr, 1965; McGarr and Vorhis 1968; Barberopoulou et al. 2006; Barberopoulou et al, 2023). Most of them are linked to distant earthquakes. In contrast, seiches associated with local earthquakes have only been documented in few publications with some of the largest collection of observations documented by Barberopoulou et al (2004; 2023) for Washington state in the U.S. and for the Kahramanmaraş, Turkey earthquake (M7.8, 6 Feb 2023). The latter is also the only dataset of seiche observations known for the Eastern Mediterranean to-date. More recently, the widespread availability of smartphones with high-resolution cameras, the use of private security cameras, and the extensive presence of swimming pools in both residential and commercial areas have enabled more frequent observations of this phenomenon. Observations of seismic seiches in lakes and other natural water bodies are scarce, mainly because data collection is sporadic. This is due to the need for a witness to be present at the time of the event, which must usually occur during daylight hours in frequently visited locations. When analyzing the geographical distribution of these observations, the location of lakes and ponds in and around the epicentral region must also be considered. This article explores the idea of using swimming pools as recording devices for this phenomenon.

## 2. The Earthquake and its Impact

On March 28, 2025, at 06:20:52 (UTC), a powerful M7.7 strike-slip supershear earthquake struck Central Myanmar near Mandalay, the country’s second-largest city

(U.S. Geological Survey 2025). The epicenter as determined by the USGS was located at 22.001°N, 95.925°E on the Sagaing Fault, a major 1400 km-long transform fault that runs down the center of Myanmar (Tun and Watkinson, 2017). Many of the country's cities—including Yangon, Naypyidaw, and Mandalay—are situated along this fault in the eastern plains between the Shan Mountains and the Irrawaddy River. The Burma and Sunda plates slide past each other at a rate of 18–49 mm per year, and the Sagaing Fault is Myanmar's largest and most active seismic source (Wang et. al, 2011). Eleven minutes after the first earthquake, a M6.7 aftershock struck with an epicenter approximately 32km to the south at 21.698°N, 95.969°E (U.S. Geological Survey 2025).

The maximum intensity reached IX - X (Extreme) on the Modified Mercalli scale (MMI, USGS; Shake USGS; Map Fig.1). The epicenter was situated in the city of Mandalay (USGS, 2025a)., Myanmar's second largest city with a population of at least 1.2 million people (Myanmar's 2024 Census Provisional Results, 2025). The disaster affected over 17 million people across the region, with 9 million severely affected. The state government of Myanmar reported an official death toll of 3,770, with 5,106 injuries and 106 people missing (Peck 2025), although due to government censorship, the true number of casulaties is likely much higher (The United Nations, 2025). The vast majority of fatalities occurred in Myanmar, with deaths also reported in Thailand. The World Bank estimated structural damage at US$11 billion, representing 14% of Myanmar's GDP. This was the most powerful earthquake to strike Myanmar since March 1912 (1912-05-23, M7.9 Myanmar; U.S. Geological Survey 2025). Ongoing civil war in the country since March 2021 severely hindered disaster relief efforts and contributed to the high number of casualties (The United Nations, 2025). The conflict also made it difficult to obtain accurate casualty reports due to censorship and lack of transparency from Burmese sources (2025 Sagaing Earthquake Archive, 2025).

In addition to major impacts in Myanmar, the earthquake disproportionately affected the Bangkok region in Thailand—approximately 1,000 km from the epicenter—due to the city's unique surface geology. Bangkok is underlain by a layer of soft alluvial clay sediment, making its many high-rises especially vulnerable to ground motion from distant powerful earthquakes (e.g. Ornthammarath, 2023)

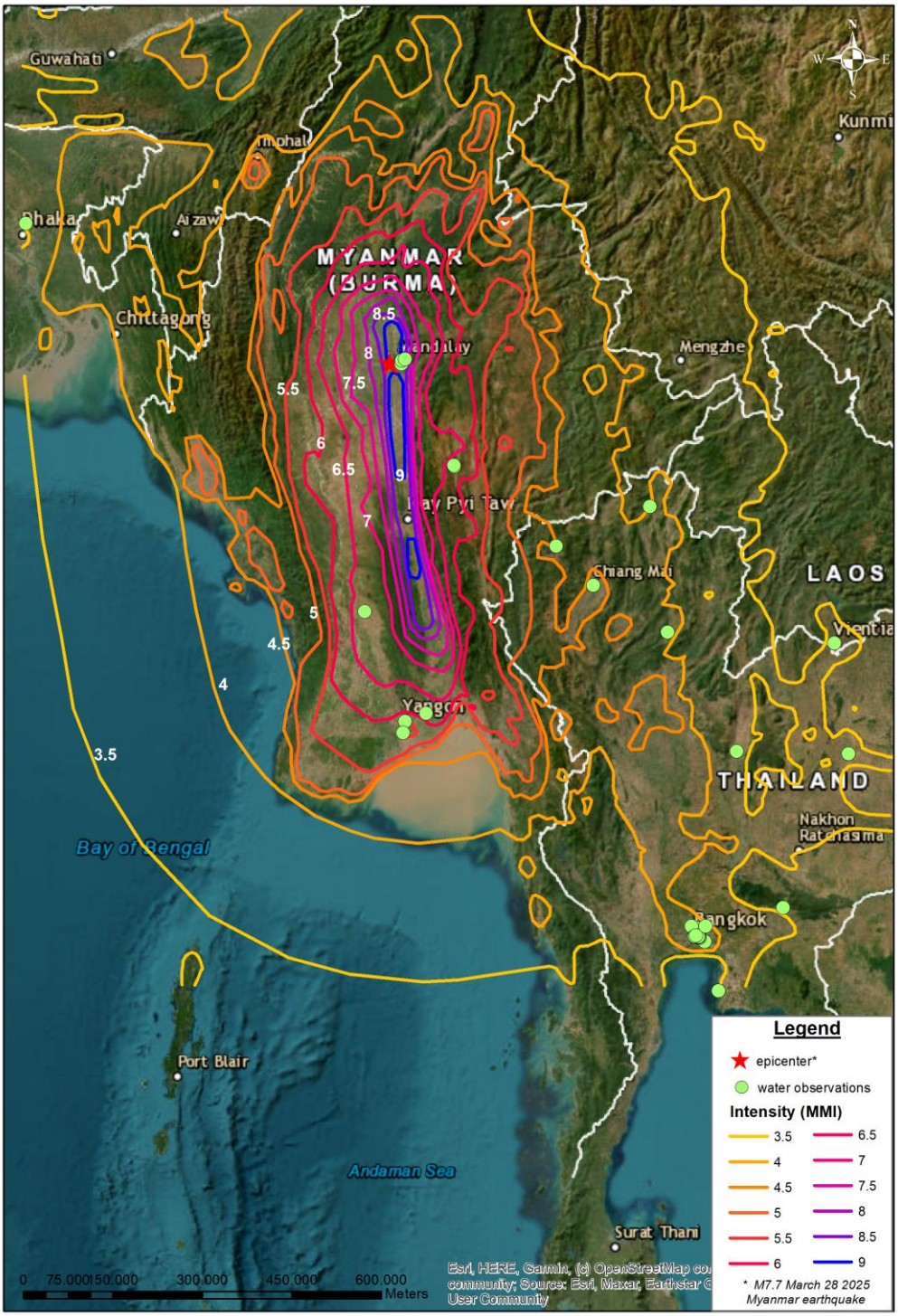


Figure 1. Intensity contours of the 28 March earthquake as reported by the USGS overlaid by observations of water waves collected for this work. Red star shows epicentral location of the March 28, 2025 Myanmar earthquake.

## 3. Materials and Data

Data in this article includes observations captured by security cameras and cellphones. Videos were found in a wide variety of social media platforms such as YouTube, Tik Tok, Instagram and X. The primary search engine terms (in English) used to find observations included combinations of “earthquake,” “waves,” “pools,” “rooftop,” “shaking,” “water” and “pond,” and other related terms. Search results were limited to those shortly after 28 March 2025 to identifying these observation videos as a record of the effects of the March 28, Myanmar earthquake. Additionally, geographic specific search terms such as the name of the country or town were also included as necessary. In addition to searching for videos filmed in Myanmar, online searches were conducted in the appropriate native languages of Myanmar and neighboring countries, including but not limited to Thai, Burmese, Lao, Vietnamese, and Bengali. Google Translate was the translation service utilized.

The collection methodology followed for this unique collection of observations follows next:

1. **Identifying Videos**: Various social media platforms were searched that integrate video, including but not limited to YouTube, Facebook, TikTok, Instagram, and X.
    a. Only seiche events documented by at least one video clearly depicting the wave directly were included in the dataset. Seiches with recordings that showed only peripheral effects, such as water spilling down structures, provided limited information for future analyses and were not included in this dataset.
2. **Verifying** links to March 28 Myanmar earthquake: Videos should be posted after March 28 and ideally within a few days of the earthquake. In nearly all cases, contextual clues were used to ensure the recordings captured the mainshock M7.7 event, not the M6.7 aftershock, as there was a noticeable calm in both people and the environment preceding the seiches.
3. **Location Determination:** Video locations were determined using various methods:
    a. Direct Information: Some videos included the location directly in the description.
    b. Identifiable features: Some videos had easy to identify landmarks in the

background, e.g. the MahaNakhon skyscraper in Bangkok.

c. Public Addresses: Other videos were posted on official business social media accounts that were linked to a public address.
d. Account Holder's Location: For videos with limited details, we often identified the location based on the account holder's general whereabouts, as indicated either explicitly on the account information or through other videos posted under the same account.
e. User Comments: In some instances, additional clues for correctly identifying the location were found in the comments.
f. If the location could not be identified with a reasonable degree of confidence and accuracy (minimum city/town or general district), the observation was excluded from the dataset.

4. **Geographical location** (latitude and longitude) and other identifying information were assigned to each observation based on available address or other location information.
    a. Identified locations were verified by looking at Google Street View as available, photos from the business's website if applicable (e.g. for hotels and restaurants), and all other public photos associated with the address on Google Maps

The above process yielded a dataset of 35 unique observations with confirmed location data (Table 1, Figures 1 & 2). Events listed under the same ID number (for example, 4.1, 4.2, etc.) represent multiple angles of a single event at one location and are not counted as unique. For each entry, the dataset details the geographical information—including city, country, latitude, and longitude—along with location accuracy (exact or approximate) and a description of the water basin where the seiching occurred (e.g., lake or rooftop pool). Due to space constraints, not all attributes are shown in the table.

This dataset does not necessarily represent all seiches that occurred throughout the region. Charts and maps only show locations where seiches were captured on video. If a seiche was observed in one body of water, it's reasonable to infer that nearby bodies of water of similar size likely experienced seiches as well—even if they weren't caught on camera.

### 3.1 Attribute Descriptions

**ID**: assigns a unique identification number to each observation. In the case of multiple videos of the same observation, this is marked as x.1, x.2, x.3, etc.

**Country**: country in which the seiche was observed

**City**: city or town in which the seiche was observed

**Lat, Long**: geographic location of where seiche was observed

**Loc. accuracy**: location information could be determined with high confidence and precision (exact) or moderate (approximate).

**Description**: identifying details about the seiche observation, including what type of body of water, etc.

**Recording device**: specifies what type of recording device was used (e.g. cellphone camera, CCTV, etc.)

**Slosh behavior**: additional informative data about water movement (not shown on this table)

**Table 1. Water observations associated with the M7.7 March 28, 2025 Myanmar earthquake**

| ID | Country | City | Lat | Long | Loc. accuracy | Description | Video Type |
|---|---|---|---|---|---|---|---|
| **1** | Thailand | Samut Prakan | 13.6504776 | 100.67986 | Exact | Rooftop pool on a skyscraper | Cellphone |
| **2** | Thailand | Sukhumvit, Bangkok | 13.70671 | 100.59981 | Exact | Rooftop pool on hotel skyscraper. Pool not very clearly shown as camera pans around, but can still see seiche movement at times in video | Cellphone |
| **3** | Thailand | Chatuchak, Bangkok | 13.82659 | 100.56717 | Exact | Rooftop pool on hotel skyscraper. In pool are floating pillows, some of which flow over | CCTV |
| **4.1** | Thailand | Pathum Wan, Bangkok | 13.7469 | 100.52897 | Exact | Rooftop pool on a hotel skyscraper. Taken from someone sitting on chair outside of pool. | Cellphone |
| **4.2** | Thailand | Pathum Wan, Bangkok | 13.7469 | 100.52897 | Exact | Rooftop pool on a hotel skyscraper. Taken from someone sitting on chair outside of pool. | Cellphone |
| **4.3** | Thailand | Pathum Wan, Bangkok | 13.7469 | 100.52897 | Exact | Rooftop pool on a hotel skyscraper. Taken from someone sitting on chair outside of pool. | Cellphone |
| **4.4** | Thailand | Pathum Wan, Bangkok | 13.7469 | 100.52897 | Exact | Rooftop pool on a hotel skyscraper. Taken from someone sitting on chair outside of pool. | Cellphone |
| **5** | Myanmar | Koksu | 16.9680313 | 96.4818259 | Exact | Water sloshes in what is presumably a fish farm open pool | Cellphone |

| | | | | | | | |
|---|---|---|---|---|---|---|---|
| **6** | Thailand | Chiang Mai | 18.8021702 | 98.9993307 | Approximate | Ground level pool in personal home | CCTV |
| **7** | Thailand | Pattaya | 12.9309639 | 100.882261 | Exact | Taken from water level on a rooftop pool | Cellphone |
| **8** | Thailand | Bang Rak, Bangkok | 13.7262607 | 100.526874 | Exact | L shaped pool on rooftop | Cellphone |
| **9** | Vietnam | Hanoi | 21.0166887 | 105.83146 | Approximate | Fish tank in office | Cellphone |
| **10** | Thailand | Chiang Rai | 19.9198413 | 99.8483288 | Approximate | Several small fish tanks | CCTV (recorded on iPad) |
| **11** | Thailand | Phetchabun (town) | 16.4205357 | 101.160636 | Approximate | Fish tank in a personal home with gold fish | Cellphone |
| **12** | Thailand | Khet Chatuchak, Bangkok | 13.8498149 | 100.567673 | Exact | Public large ground level swimming pool | Cellphone |
| **13** | Myanmar | Mandalay | 21.9278214 | 96.1080981 | Approximate | Personal rooftop pool at private home | CCTV |
| **14** | Thailand | Pai city, Mae Hong Son province | 19.3587896 | 98.4372542 | Approximate | Personal background pool at ground level | CCTV |
| **15** | Myanmar | Nattalin | 18.4248062 | 95.5591082 | Exact | Pond in rural area | CCTV |

| | | | | | | | |
|---|---|---|---|---|---|---|---|
| **16** | Myanmar | Inle Lake | 20.4875978 | 96.9051996 | Approximate | Lake upon which are situated houses on stilts (famous "floating villages") | Cellphone |
| **17** | Thailand | Khon Kaen province | 16.3809968 | 102.845767 | Exact | Large Shrimp pond in center of restaurant | CCTV |
| **18** | Thailand | Phae Province | 18.1341342 | 100.117836 | Exact | Khoi pond or similar sloshes around flooding restaurant | Cellphone |
| **19** | Myanmar | Yangon (a.k.a Rangoon) | 16.8470287 | 96.1637198 | Approximate | Water in bubbler plastic water holder swishes back and forth | Cellphone |
| **20** | Myanmar | Mandalay | 21.9742823 | 96.1184641 | Exact | Violent shaking in medium fish tank in spa | CCTV |
| **21** | Bangladesh | Dhaka | 23.8741471 | 90.4558927 | Approximate | Pond, small movement | Cellphone |
| **22** | Myanmar | Patheingyi | 21.9951314 | 96.162847 | Approximate | Violent shaking in ground level pool | Cellphone |
| **23** | Vietnam | Long An | 10.5430036 | 106.406968 | Exact | Some sort of fish pond in center of restaurant | CCTV |
| **24** | Myanmar | Yangon (a.k.a Rangoon) | 16.685195 | 96.1347726 | Approximate | Roadside ditch | Cellphone |
| **25** | Myanmar | Inle Lake | 20.5041287 | 96.9037099 | Approximate | House floating on stilts shakes | Cellphone |
| **26** | Laos | Vientiane | 17.97698 | 102.632003 | Approximate | Ground level (?) pool in personal backyard | CCTV |
| **27** | Vietnam | Hanoi | 21.0211323 | 105.821531 | Approximate | Fish tank in personal home | Cellphone |

| | | | | | | | |
|---|---|---|---|---|---|---|---|
| **28** | Thailand | Bangkok | 13.7165547 | 100.58501 | Exact | Extremely violent shaking on rooftop pool | Cellphone |
| **29** | Thailand | Nonthaburi | 13.8737704 | 100.479168 | Exact | Seiche viewed from another nearby rooftop | Cellphone |
| **30** | Thailand | Bangkok | 13.7250924 | 100.525231 | Exact | Seiche on floor 20 of hotel. Unique motion creates standing wave with multiple peaks. | Cellphone |
| **31.1** | Thailand | Bangkok | 13.7224147 | 100.581341 | Exact | Seiche on rooftop pool of hotel. View from above pool level, allowing to see seiche directly. | Cellphone |
| **31.2** | Thailand | Bangkok | 13.7224147 | 100.581341 | Exact | View of previous observation from adjacent apartment building. Can see water spilling down off the edges. | Cellphone |
| **31.3** | Thailand | Bangkok | 13.7224147 | 100.581341 | Exact | Video of previous observation from ground level | Cellphone |
| **32** | Thailand | Bangkok | 13.7263033 | 100.526886 | Exact | L shaped pool on rooftop | Cellphone |
| **33** | Thailand | Bangkok | 13.7390346 | 100.545124 | Exact | Backyard pool at ground level at the Dutch Embassy | Cellphone |
| **34** | Thailand | Bangkok | 13.8780358 | 100.690773 | Approximate | Ground level pool in private residence | Cellphone |
| **35** | Thailand | Na Di | 14.149498 | 101.854829 | Approximate | Pond next to road with large waves | Cellphone |

## 4. Results

A total of 39 water observations were collected from various countries linked to the March 28 Myanmar earthquake. Of these, 35 were from unique locations that were identified with a high degree of confidence. A sample of the kind of observations collected (still images from videos) were mosaicked for Figure 2.

We created various maps and charts to visualize the data and identify patterns in the observation distribution. A map of observations collected (white circles), overlay countries with observations (colored polygons) in Figure 3. This map illustrates the geographic distribution of observations by water body type. Three inset maps are provided, with clusters of observations shown near the earthquake's epicenter in Mandalay and Yangon, Myanmar, as well as in Bangkok, Thailand. Observations have also been grouped by country and by category (Fig.4). Based on our collection of data, most observations were collected from Thailand. Most observations were from manmade water basins, and especially rooftop pools specifically. A few observations were collected from natural water basins (lakes; Fig.4). Videos from swimming pools tend to show clear side to side motion along the short side of pools especially in Thailand. Water motions from closer-to-the-epicenter locations show more complex water motion.

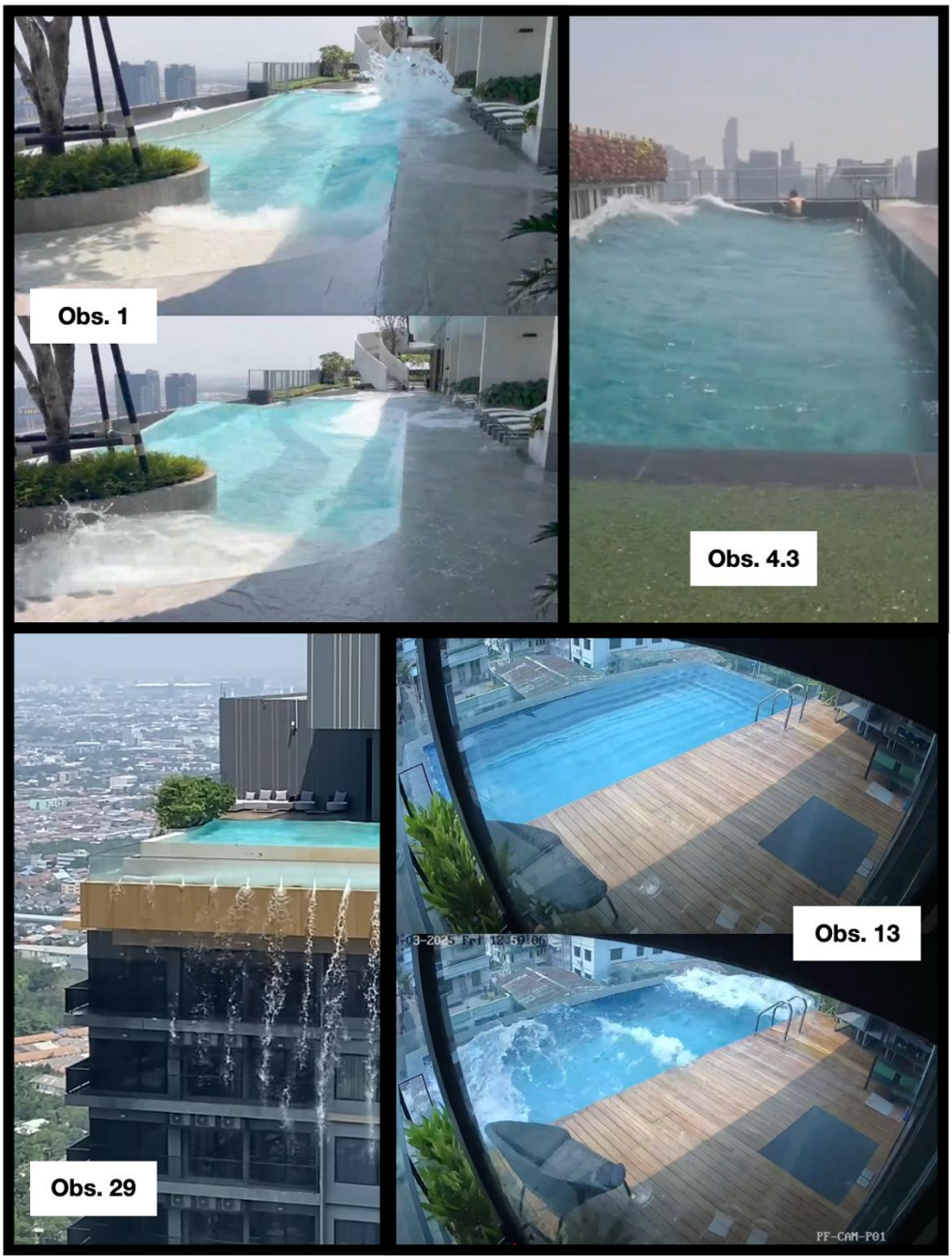


Figure 2. Selected still images captured from various videos in the dataset show water motion in small bodies of water. Observation 1 shows water sloshing in a rooftop pool on a skyscraper in Thailand, where the water moves from side to side along the pools' shorter side. Observation 4.3 shows similar side to side motion from another rooftop pool. The first frame of Observation 13 was taken just after ground shaking began and shows a complex wave motion. A few seconds later, the second frame shows violent splashing, first along the long side and then later (not shown) along the short. Observation 29 shows water sloshing from side to side along the width of a swimming pool in Nonthaburi, Thailand. Spilling from rooftop swimming pools was a unique characteristic of earthquake effects in this earthquake.

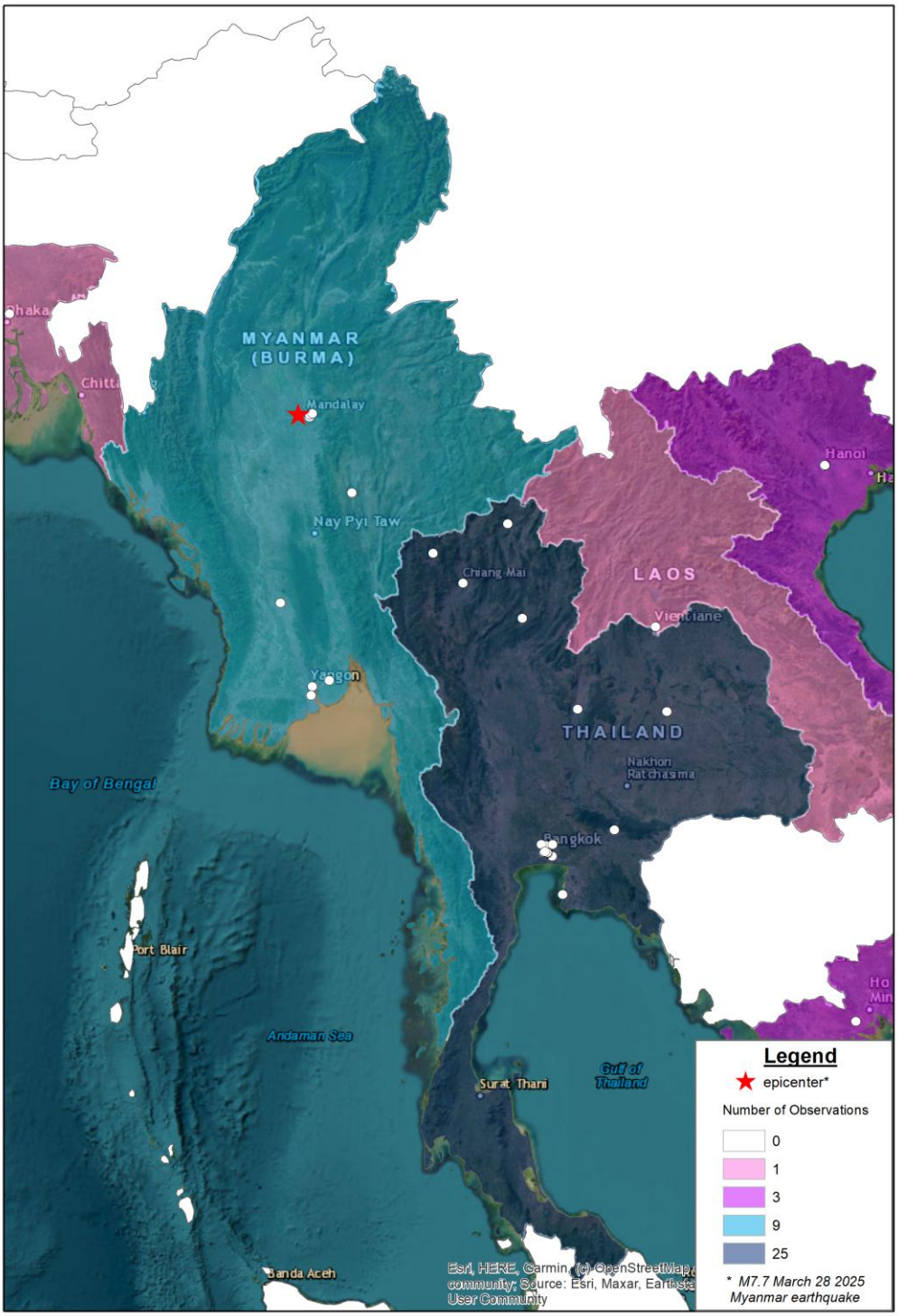


Figure 3 Set of unique observations (white circles) collected after the March 28, Myanmar M7.7 earthquake. Countries with observations appear colored according to number of observations (the darker the shade the more observations).

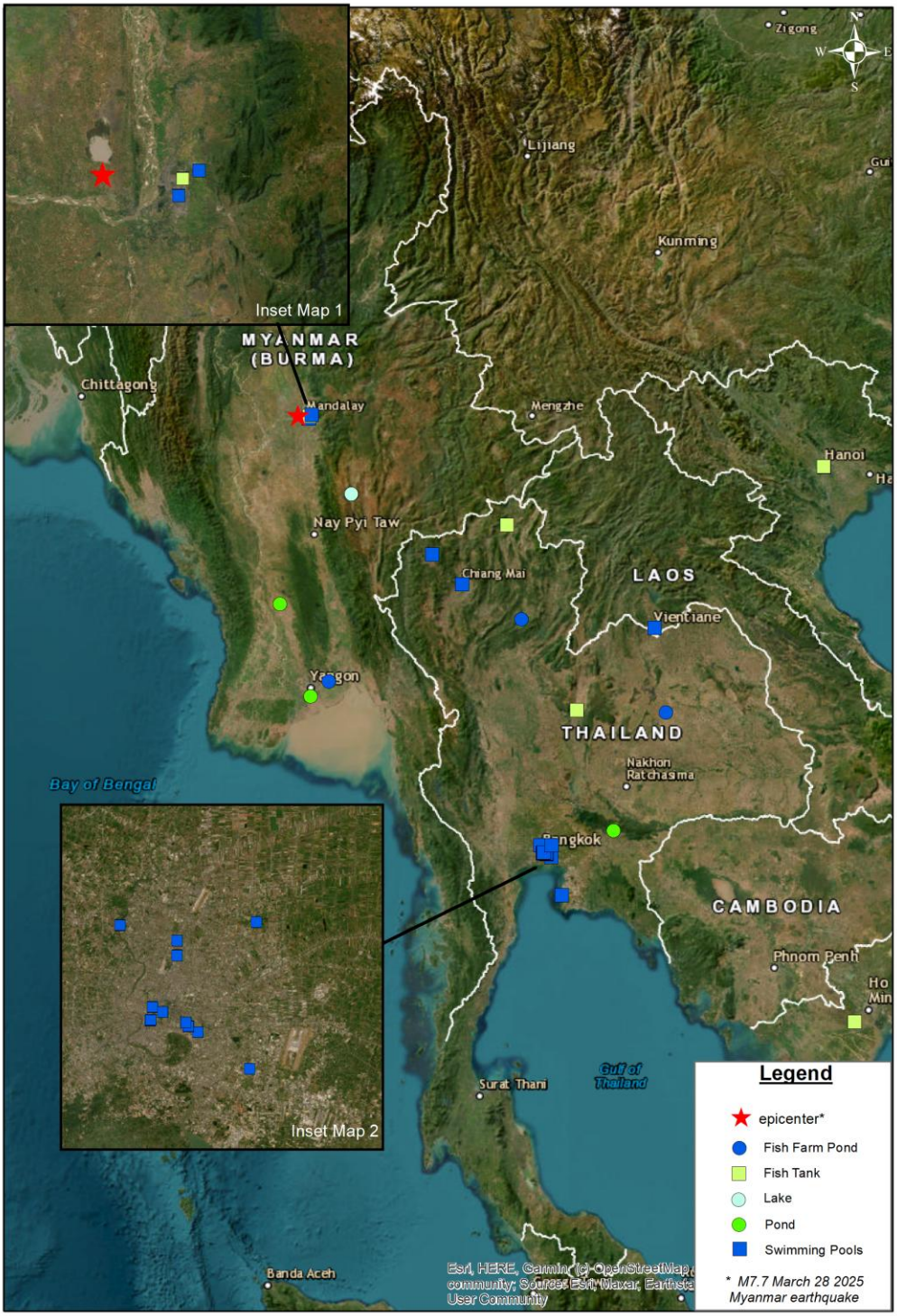


Figure 4. Geographic distribution of observations by type of body of water. Inset maps (from top to bottom) show clusters of observations nearby the epicenter in Mandalay, Myanmar; in Yangoon, Myanmar; and in Bangkok, Thailand.

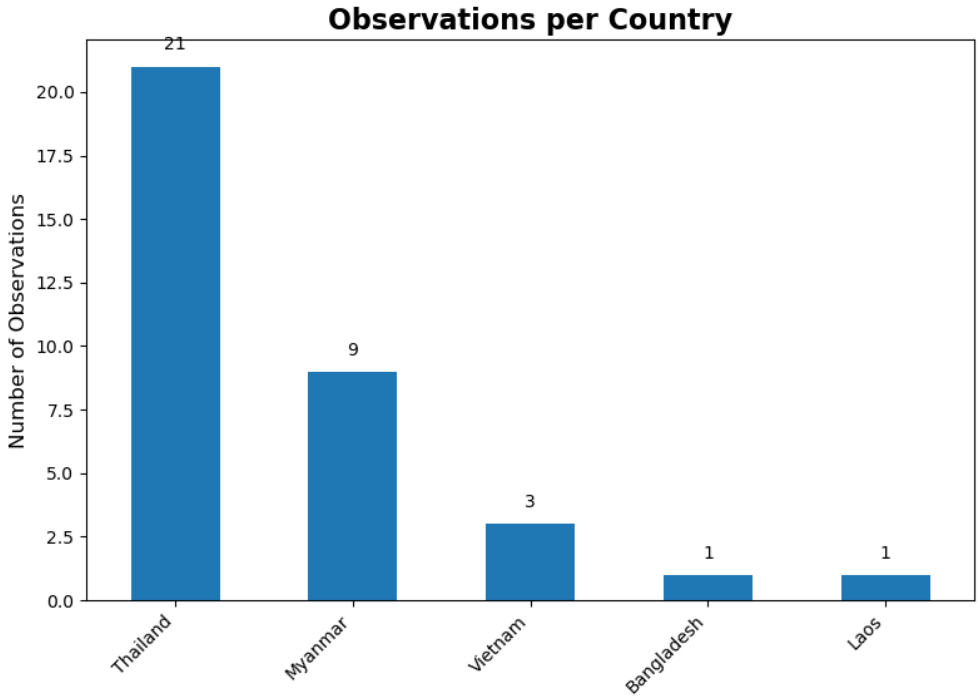


Figure 5. Unique observations grouped by country.

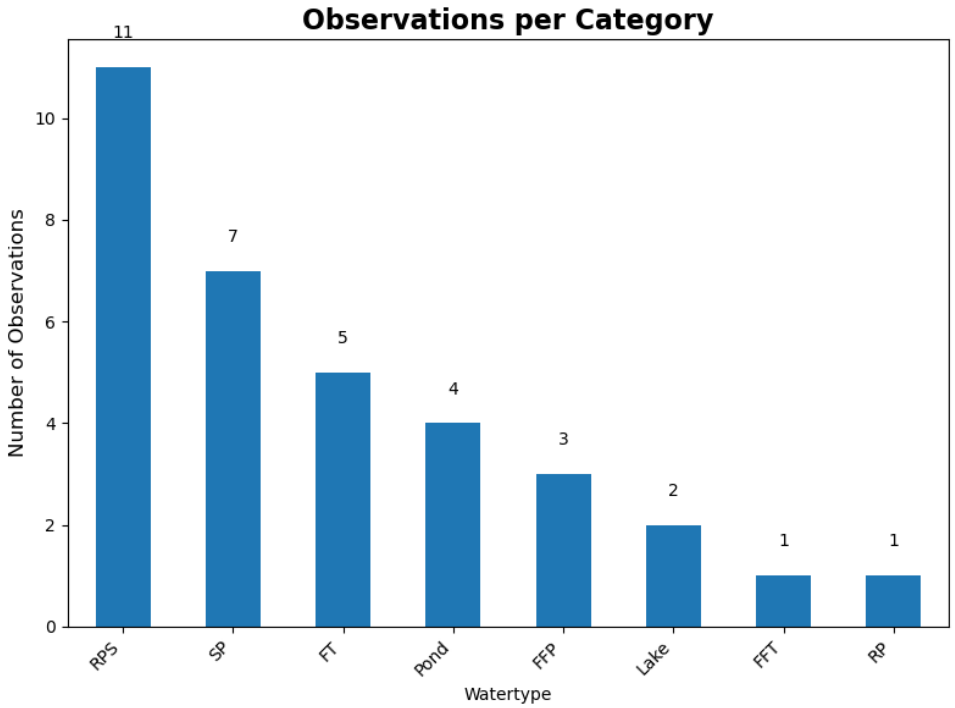


Figure 6. Eight categories were used to group observations from similar settings. Abbreviated names correspond to, Rooftop Pools on Skyscrapers (RPS), Rooftop Pools (RP) for rooftop pools on other buildings, Swimming Pools (SP) for other pools such as residential pools on the ground, Fish Tanks (FT) and Fish Farm Ponds (FFP) and Fish Farm Tanks (FFT).

## 5. Discussion and Conclusions

On March 28, 2025 a M7.7 struck Mandalay city in Myanmar. The impact of the earthquake was quite severe with at least 3,700 deaths, many collapsed buildings and damaged infrastructure. Due to censorship the number of fatalities and destructed buildings may be larger. The earthquake impacted also neighboring countries such as Thailand in locations as far as 1000km. One of the "identifying" seismic effects of this earthquake was the spilled water over skyrise buildings which was a result of sloshing initiated in rooftop pools as a result of earthquake ground motions. This phenomenon also known as seismic seiching was the focus of our paper. Specifically, a total of 39 (35 unique) water observations with locations confidently identified were collected from various countries that are associated with the March 28, Myanmar earthquake. The unique video collection associated with the observations listed in this article from various water basins (fish tanks to lakes), resembled an experiment of water wave generation in different settings under seismic shaking.

Although the epicenter was in Myanmar, most of the observations were from Thailand likely a result of bias. More specifically, Bangkok's surface geology renders it particularly sensitive to ground movement (e.g., Ornthammarath et al., 2023). This sensitivity, alongside the city's abundance of high-rise buildings, rooftop pools, and security cameras, provides a logical explanation for why a majority of our observations originate from Bangkok despite the epicenter being in Myanmar. More importantly, this study is in line with previous findings that large sedimentary basins exert a strong control on the location where these observations occur (McGarr, 1965; McGarr and Vorhis, 1968; Barberopoulou et al., 2004, 2006).

This paper's primary aim was the systematic documentation and preservation of this unique dataset, alongside some basic analysis of the findings. While a full, comprehensive analysis is planned for a future study, the fundamental question we seek to address is whether the collected observations, through this meticulous documentation, can yield new insights that advance our understanding of seismic seiche waves.

## 6. References


2025 Sagaing Earthquake Archive. (n.d.). *[Channel post]*. YouTube. http://youtube.com/post/Ugkx45OF3PKsnI7MsT19ahpZkNJTav_1DSag?si=z6SLqSAlA1HhoDAI

Barberopoulou, A. (2006). Long-Period Effects of the Denali Earthquake on Water Bodies in the Puget Lowland: Observations and Modeling. *Bulletin of the Seismological Society of America*, *96*(2), 519–535. https://doi.org/10.1785/0120050090

Barberopoulou, A., Malaperdas, G., & Firth, S. (2023). COASTAL EFFECTS, Tsunami And Seiching Associated With The Kahramanmaraş Turkey-Syria Twin Earthquakes And Aftershock Sequence Of February 2023. *Science of Tsunami Hazards*, *42*(3), 257-272.

Barberopoulou, A., Qamar, A., Pratt, T. L., Creager, K. C., & Steele, W. P. (2004). Local amplification of seismic waves from the Denali Earthquake and damaging seiches in Lake Union, Seattle, Washington. *Geophysical Research Letters*, *31*(3), 2003GL018569. https://doi.org/10.1029/2003GL018569

Bondevik, S., Gjevik, B., & Sørensen, M. B. (2013). Norwegian seiches from the giant 2011 Tohoku earthquake. *Geophysical Research Letters*, *40*(13), 3374–3378. https://doi.org/10.1002/grl.50639

Canitano, A., Bernard, P., & Allgeyer, S. (2017). Observation and modeling of the seismic seiches triggered in the Gulf of Corinth (Greece) by the 2011 Mw 9.0 Tohoku earthquake. *Journal of Geodynamics*, *109*, 24–31. https://doi.org/10.1016/j.jog.2017.06.001

Forel, F.-A. (1876). *Les Seiches, vagues d'oscillation fixe des lacs*. *83*, 712–714.

Korgen, B. J. (1995). Seiches: transient standing-wave oscillations in water bodies can create hazards to navigation and unexpected changes in water conditions. *American Scientist*, *83*(4), 330+. Gale Academic OneFile. https://link.gale.com/apps/doc/A166995659/AONE?u=anon~3d01e2b4&sid=googleScholar&xid=1afdd1d3

Kvale, A. (1955). Seismic seiches in Norway and England during the Assam earthquake of August 15, 1950*. *Bulletin of the Seismological Society of America*, *45*(2), 93–113. https://doi.org/10.1785/BSSA0450020093

McGarr, A. (1965). Excitation of seiches in channels by seismic waves. *Journal of Geophysical Research*, *70*(4), 847–854.

https://doi.org/10.1029/JZ070i004p00847

McGarr, A., & Vorhis, R. C. (1968). *Seismic Seiches from the March 1964 Alaska Earthquake* (No. U.S. Geological Survey Professional Paper 544–E; p. 43). United States Geological Survey. https://pubs.usgs.gov/pp/0544e/

Myanmar's 2024 Census Provisional Results: Population at 51.3M. (2025). *The Global New Light of Myanmar*. https://www.gnlm.com.mm/myanmars-2024-census-provisional-results-population-at-51-3m/

Omer, S. (2025, May 23). Myanmar earthquake: Facts, FAQs, and how to help. *World Vision*. https://www.worldvision.org/disaster-relief-news-stories/myanmar-earthquake-facts-faqs-how-to-help

Ornthammarath, T., Jirasakjamroonsri, A., Pornsopin, P., Rupakhety, R., Poovarodom, N., Warnitchai, P., & Toe, T. T. T. (2023). Preliminary analysis of amplified ground motion in Bangkok basin using HVSR curves from recent moderate to large earthquakes. *Geoenvironmental Disasters*, *10*(1), 28. https://doi.org/10.1186/s40677-023-00259-0

Peck, G. (2025). Humanitarian needs remain pressing a month after Myanmar's deadly quake. *The Associated Press*. https://apnews.com/article/myanmar-quake-humanitarian-red-cross-un-civil-war-2c1f6af0f36df1332647185b42ae2e2d

Rabinovich, A. B. (n.d.). Seiches and Harbor Oscillations. In *Handbook of Coastal and Ocean Engineering* (pp. 193–236). https://doi.org/10.1142/9789812819307_0009

The United Nations. (2025, April 10). UN expert calls for emergency Security Council action to address ceasefire violations after devastating Myanmar earthquake. *Office of the High Comissioner*. https://www.ohchr.org/en/press-releases/2025/04/un-expert-calls-emergency-security-council-action-address-ceasefire

Tun, S. T., & Watkinson, I. M. (2017). Chapter 19: The Sagaing Fault, Myanmar. In *Myanmar: Geology, Resources and Tectonics* (Vol. 48). The Geological Society of London. https://doi.org/10.1144/M48.19

U.S. Geological Survey, Earthquake Hazards Program. (2025a). *M 7.7 - 2025 Mandalay, Burma (Myanmar) Earthquake*. M 7.7 - 2025 Mandalay, Burma (Myanmar) Earthquake - Technical. https://earthquake.usgs.gov/earthquakes/eventpage/us7000pn9s/technical

U.S. Geological Survey, Earthquake Hazards Program. (2025b). *M 7.9 - 32 km NW of Taunggyi, Myanmar*.

U.S. Geological Survey, Earthquake Hazards Program, Earthquake Hazards Program. (2025). *M 6.7 - Burma (Myanmar)*. https://earthquake.usgs.gov/earthquakes/eventpage/us7000pn9z/executive

Wang, Y., Sieh, K., Aung, T., Min, S., Khaing, S. N., & Tun, S. T. (2011). Earthquakes and slip rate of the southern Sagaing fault: insights from an offset ancient fort wall, lower Burma (Myanmar). *Geophysical Journal International*, *185*(1), 49–64. https://doi.org/https://doi.org/10.1111/j.1365-246X.2010.04918.x

Wilson, B. W. (1972). *Seiches* (V. T. CHOW, Ed.; Vol. 8, pp. 1–94). Elsevier. https://doi.org/10.1016/B978-0-12-021808-0.50006-1

ISSN 8755-6839

SCIENCE OF TSUNAMI HAZARDS

The Journal of Tsunami Society International

Volume 43 Number 2 2025

# Tsunamis in Antarctica, a statistical analysis

*R. Kh. Mazova, [1,*], N. A. Zhukov[1], E.F Denisov[1]*

[1] *Nizhny Novgorod State Technical University n.a. R.E. Alekseev, 24, Minin str., 603155 Nizhny Novgorod, Russia*

***** R. Kh. Mazova, E-mail: raissamazova@yandex.ru

**Abstract**

This study investigates earthquake activity in the Antarctic region, analyzing data spanning from 1980 to 2024 (M ≥ 5.0, with a maximum recorded magnitude *M*=8.1). Utilizing a dataset bounded by the 50th southern parallel, the research focuses on constructing and examining the Gutenberg–Richter recurrence law. Using the normal distribution law and the lognormal distribution, graphs of the normal distribution of earthquake magnitudes and the recurrence law of earthquake magnitudes for the Antarctic region for the period under consideration are constructed. This analysis provides crucial insights into the seismicity patterns of the Antarctic region.

**Keywords*:*** Antarctic region, earthquakes and aftershocks, normal distribution, recurrence law.

## 1. Introduction

Antarctica was first discovered in 1820 during the first Russian Antarctic expedition (Russia in colors, 2004-2015). The first, successful landing on the continent took place in 1895, and less than half a century later, seismological research had already begun in the region. Research stations began to appear starting in 1898. Fig. 1 clearly shows the pattern of earthquakes and their aftershocks at the boundaries of lithospheric plates (Fig.1) (Bellingshausen, 1949; Antarctic stations, 2025). A large number was recorded, including some of the strongest tsunamis associated with M>7.0 earthquakes, at the boundaries of the Scotia plate, as well as in the area of the southern boundary of the Australian plate (Fig. 2) (Antarctic stations, 2023).

The Antarctic plate, which completely surrounds the continent, also borders 6 plates of the predominantly southern hemisphere. Fig. 2 shows the directions of lithospheric plate motions relative to each other (Reading, 2007). In August 2021, one of the strongest earthquakes in Antarctic history occurred along the eastern boundary of the Scotia Plate, near the South Sandwich Islands, with a maximum magnitude of *M* = 8.1 (Russia in Colors, 2004-2015; Antarctic Stations, 2023)

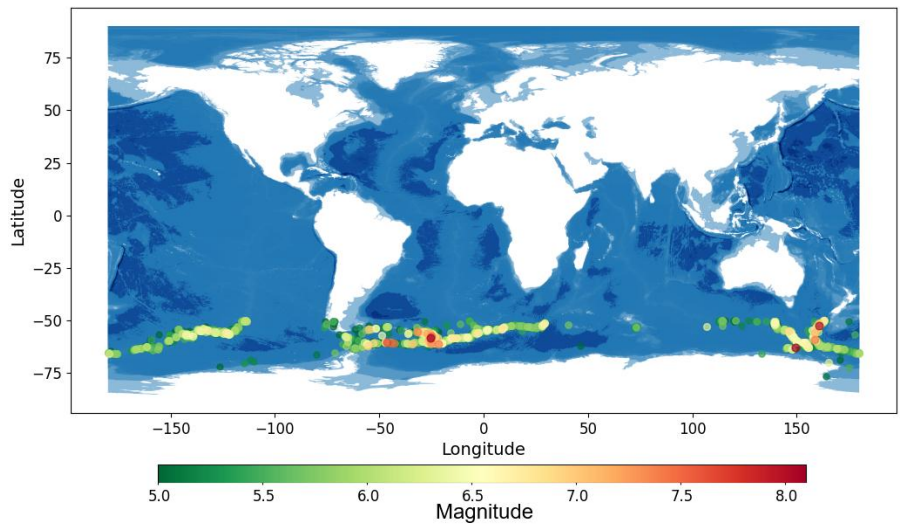


Figure 1. Earthquakes and aftershocks in the Antarctic region from 1980 to 2024 with M > 5.0, according to NEIC and ISC data (Bellingshausen, 1949; Antarctic stations, 2023 and references therein).

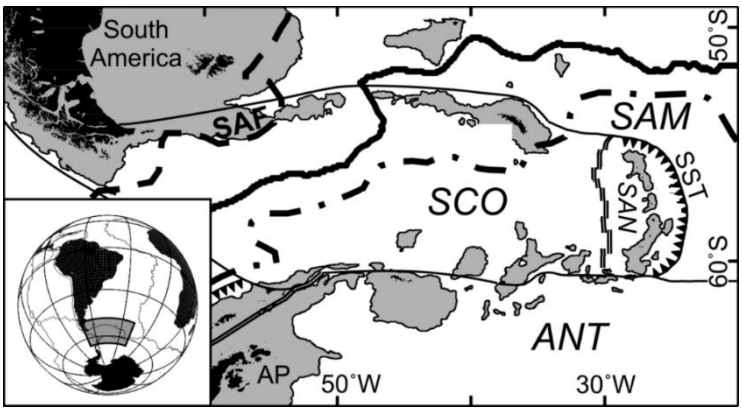


Figure 2. Plate movement process: the Scotia Sea showing the ESR in relation to the Scotia Plate (SCO), South Sandwich Plate (SAN), South American Plate (SAM), the Antarctic Plate (ANT), the Antarctic Peninsula (AP), and the South Sandwich Trench (SST) (Bellingshausen, 1949; Antarctic stations, 2023).

## 2. Data and Methods

Earthquake and aftershock data for the marine Antarctic region were analyzed (The U.S. Geological Survey, 1879; International Seismological Centre, 1964; Reading, 2007). This study focused on events within the geographical boundary of the 50th southern parallel, spanning the period from the beginning of 1980 to 2024. A magnitude threshold of M ≥ 5.0 was applied, with the highest recorded magnitude during this interval being M = 8.1. For each seismic event, a comprehensive database was compiled, including coordinates, exact time, and magnitude. The process of constructing the Gutenberg–Richter recurrence law (Dubinin, 2006; SCALING LAWS, n.d.) was then examined. This fundamental law describes the relationship between the number of earthquakes and their respective magnitudes. (equation 1)

$$logN = a - bM \quad (1)$$

where *N* is the number of events; *M* is magnitude; and a, b are constants that depend on the activity of the selected region.

To construct the recurrence law, all tremors (earthquakes and aftershocks) were grouped by their corresponding main earthquakes or strong aftershocks. This grouping was achieved using approximate temporal and spatial boundaries for the aftershocks of a single earthquake (SCALING LAWS, n.d.). The Haversine formula was employed to

calculate distances on the sphere based on event coordinates ((Dubinin, 2006; equation 2).

$$d = 2r \cdot \arcsin\left(\sqrt{\sin^2\left(\frac{\varphi_2 - \varphi_1}{2}\right) + \cos\varphi_1 \cos\phi_2 \sin^2\left(\frac{\lambda_2 - \lambda_1}{2}\right)}\right), \qquad (2)$$

where $r = 6371$ is the Earth's radius in km; $\varphi_1, \varphi_2$ are latitudes in radians; $\lambda_1, \lambda_2$ are longitudes in radians.

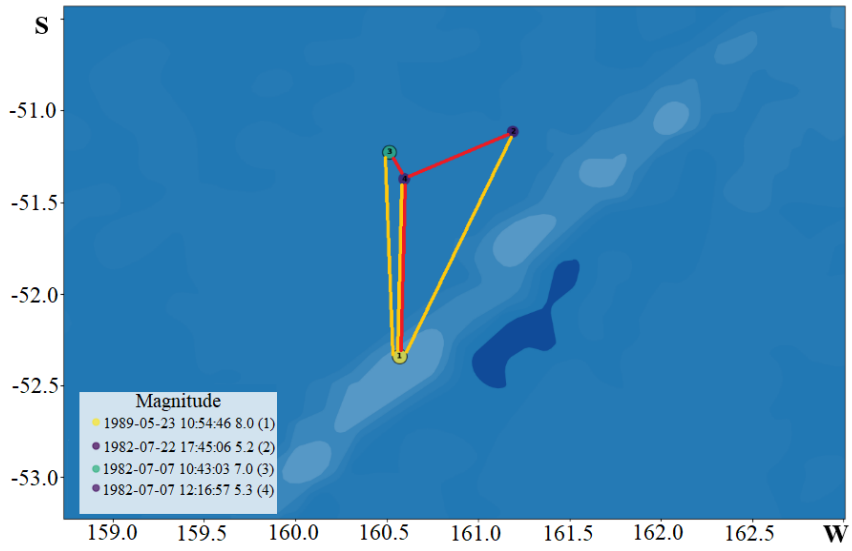


Figure 3. Graphical representation of aftershock clustering (yellow lines – inclusion within permissible scatter radius method; red lines – graph method) for the 1989 Macquarie Ridge earthquake.

Aftershocks can be linked to the initial earthquake in a specific area. This can be done in two ways: either by measuring their distance from the first earthquake alone, or, if seismic activity spreads in a chain reaction, by using a graph method to find the closest preceding shocks (Fig. 3).

We can define the boundary conditions for including an aftershock in an earthquake sequence based on these criteria (Utsu, 1961):

- **Magnitude (M) 5-6:** Aftershocks must occur within **100 km** of the mainshock.
- **Magnitude (M) >7:** Aftershocks can be included if they are within **1,000 km** of the epicenter, although there is a wider scatter in the exact values.

- **Time:** Aftershocks for the most powerful earthquakes are typically considered part of the sequence for up to **20 days** after the initial shock.

## 3. Statistical Study of Antarctic Marine Seismicity

Based on the obtained data, a statistical analysis of earthquake magnitude recurrence in the Antarctic waters was conducted. Using the normal distribution law (Utsu, 1961; Mazova et al., 1983; Ivchenko & Medvedev, 1984: equation 4) we constructed graphs for the normal distribution of earthquake magnitudes, the earthquake magnitude recurrence graph on a double logarithmic scale, and the probability of earthquake magnitude recurrence for the Antarctic region.

$$f(x) = \frac{1}{\sigma\sqrt{2\pi}} e^{-\frac{(x-\mu)^2}{2\sigma^2}} \qquad (4)$$

where $\mu$ is the expected value; $\sigma$ is the variance, and the log-normal distribution is given by equation 5 (Mazova et al., 1983; Ivchenko & Medvedev, 1984)

$$f(x) = \frac{e^{-\frac{\left(\frac{\ln x-\mu}{\sigma}\right)^2}{2}}}{x\sigma\sqrt{2\pi}} \qquad (5)$$

The sample data were grouped as detailed in Table 2 (Mazova et al., 1983; Ivchenko & Medvedev, 1984) to construct the histogram of earthquake magnitude distribution. The resulting histogram (Fig. 4) illustrates the distribution of earthquake magnitudes in the Antarctic region over the past 50 years.

Table 1. Distribution of earthquakes per magnitude

| **Magnitude** | **Point count N** | **Magnitude** | **Point count N** |
|---|---|---|---|
| M < 5.1 | 238 | 6.4 < M < 6.6 | 13 |
| 5.0 < M < 5.2 | 186 | 6.5 < M < 6.7 | 10 |
| 5.1 < M < 5.3 | 190 | 6.6 < M < 6.8 | 10 |
| 5.2 < M < 5.4 | 148 | 6.7 < M < 6.9 | 4 |
| 5.3 < M < 5.5 | 145 | 6.8 < M < 7.0 | 7 |
| 5.4 < M < 5.6 | 122 | 6.9 < M < 7.1 | 3 |
| 5.5 < M < 5.7 | 91 | 7.0 < M < 7.2 | 2 |
| 5.6 < M < 5.8 | 76 | 7.1 < M < 7.3 | 3 |
| 5.7 < M < 5.9 | 52 | 7.2 < M < 7.4 | 1 |
| 5.8 < M < 6.0 | 49 | 7.3 < M < 7.5 | 3 |
| 5.9 < M < 6.1 | 38 | 7.4 < M < 7.6 | 1 |
| 6.0 < M < 6.2 | 31 | 7.5 < M < 7.7 | 1 |
| 6.1 < M < 6.3 | 31 | 7.6 < M < 8.0 | - |
| 6.2 < M < 6.4 | 24 | 7.9 < M < 8.1 | 1 |
| 6.3 < M < 6.5 | 22 | 8.0 < M | 1 |

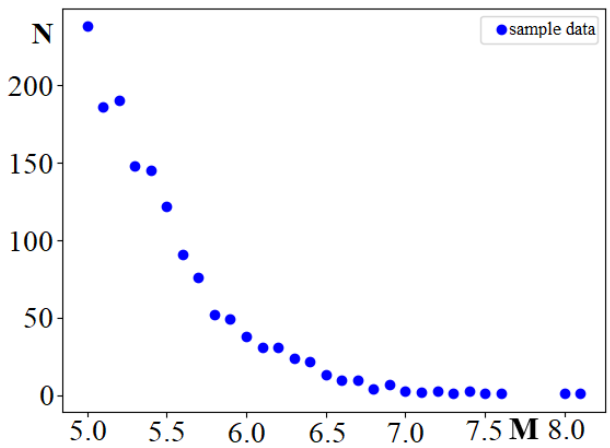


Figure 4. Histogram of earthquake magnitude distribution in the Antarctic region. Blue dots represent the sample data for the presented magnitude values (Table 1).

Earthquake data (Table 1) was processed to estimate the recurrence of earthquake magnitudes. The purpose of this step was to normalize the data and prepare

it for distribution analysis. Table 2 shows these normalized values, which were calculated by dividing the number of sample points for each magnitude by the total number of samples. This normalization allows for a direct comparison of the relative frequency of earthquakes across different magnitude ranges.

The results of this analysis are presented in Figure 5, which shows the recurrence of earthquake magnitudes on both linear and double logarithmic scales. The normal distribution approximation curve is represented by the blue and red lines. The right side of the graph is specifically described by formula (4), using the coefficients calculated from the data.

Table 2. Data for constructing the earthquake magnitude distribution histogram in the Antarctic Region

| **Magnitude** | **Point count N** | **$N/N_{totl}$** | **Magnitude** | **Point count N** | **$N/N_{totl}$** |
|---|---|---|---|---|---|
| M < 5.1 | 238 | 1 | 6.4 < M < 6.6 | 13 | 0.055 |
| 5.0 < M < 5.2 | 186 | 0.78 | 6.5 < M < 6.7 | 10 | 0.042 |
| 5.1 < M < 5.3 | 190 | 0.798 | 6.6 < M < 6.8 | 10 | 0.042 |
| 5.2 < M < 5.4 | 148 | 0.62 | 6.7 < M < 6.9 | 4 | 0.017 |
| 5.3 < M < 5.5 | 145 | 0.6 | 6.8 < M < 7.0 | 7 | 0.029 |
| 5.4 < M < 5.6 | 122 | 0.51 | 6.9 < M < 7.1 | 3 | 0.013 |
| 5.5 < M < 5.7 | 91 | 0.38 | 7.0 < M < 7.2 | 2 | 0.0084 |
| 5.6 < M < 5.8 | 76 | 0.32 | 7.1 < M < 7.3 | 3 | 0.013 |
| 5.7 < M < 5.9 | 52 | 0.22 | 7.2 < M < 7.4 | 1 | 0.0042 |
| 5.8 < M < 6.0 | 49 | 0.2 | 7.3 < M < 7.5 | 3 | 0.013 |
| 5.9 < M < 6.1 | 38 | 0.16 | 7.4 < M < 7.6 | 1 | 0.0042 |
| 6.0 < M < 6.2 | 31 | 0.13 | 7.5 < M < 7.7 | 1 | 0.0042 |
| 6.1 < M < 6.3 | 31 | 0.13 | 7.6 < M < 8.0 | - | - |
| 6.2 < M < 6.4 | 24 | 0.1 | 7.9 < M < 8.1 | 1 | 0.0042 |
| 6.3 < M < 6.5 | 22 | 0.09 | 8.0 < M | 1 | 0.0042 |

Based on the processed data in Table 2, a graph illustrating the recurrence of earthquake magnitudes was plotted (Figure 5 (left)). To better visualize the distribution, this same data is also presented on a double logarithmic scale in Figure 5 (right). The

blue and red lines in the figure show the normal distribution approximation curve, with the right side of the graph being described by formula (4) using the corresponding calculated coefficients.

$$f(x)=280*e^{\frac{(\frac{x}{6.5}-0.7)^2}{0.0026}} \quad (6)$$

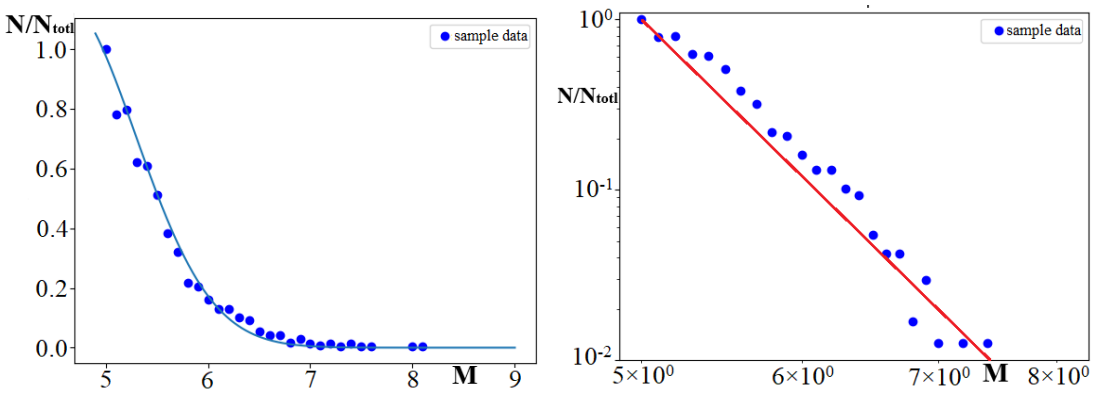


Figure 5 (left) Normal distribution of earthquake magnitudes for the Antarctic region, orthonormalized to the total number of events, and (right), graph of earthquake magnitude recurrence for the Antarctic region, orthonormalized to the total number of events, on a double logarithmic scale.

Based on the same sample data, Table 3 was compiled to show the probability of recurrence for earthquakes of a specific magnitude. The table's first column lists the magnitude intervals, starting from the minimum value. The third column provides the calculated probability that an earthquake's magnitude will fall within each respective interval.

Table 3. Earthquake recurrence probability

| Magnitude | Point count N | P | Magnitude | Point count N | P |
|---|---|---|---|---|---|
| ≤5.1 | 238 | 0.158 | ≤6.5 | 1 443 | 0.96 |
| ≤5.2 | 424 | 0.282 | ≤6.6 | 1 456 | 0.969 |
| ≤5.3 | 614 | 0.409 | ≤6.7 | 1 466 | 0.976 |
| ≤5.4 | 762 | 0.507 | ≤6.8 | 1 476 | 0.983 |
| ≤5.5 | 907 | 0.604 | ≤6.9 | 1 480 | 0.985 |
| ≤5.6 | 1 029 | 0.685 | ≤7.0 | 1 487 | 0.99 |
| ≤5.7 | 1 120 | 0.746 | ≤7.1 | 1 490 | 0.992 |
| ≤5.8 | 1 196 | 0.796 | ≤7.2 | 1 492 | 0.993 |
| ≤5.9 | 1 248 | 0.83 | ≤7.3 | 1 495 | 0.995 |
| ≤6.0 | 1 297 | 0.864 | ≤7.4 | 1 496 | 0.996 |
| ≤6.1 | 1 335 | 0.889 | ≤7.5 | 1 499 | 0.998 |
| ≤6.2 | 1 366 | 0.909 | ≤7.6 | 1 500 | 0.9987 |
| ≤6.3 | 1 397 | 0.93 | ≤8.0 | 1 501 | 0.9993 |
| ≤6.4 | 1 421 | 0.946 | ≤8.1 | 1 502 | 1 |

The recurrence probability of earthquake magnitudes for the Antarctic region is visually represented in a generated graph, based on the data in Table 3 (Figure 6). The plot features a logarithmic x-axis and includes a blue dashed line to approximate the integral curve of the normal distribution.

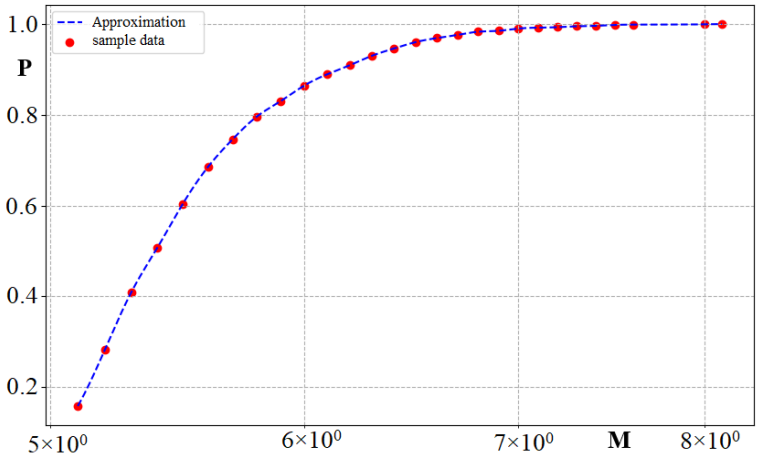


Figure 6. Graph of earthquake magnitude recurrence probability in the Antarctic region (data is from Table 4)

## 4. Conclusion

In this work, a statistical analysis was conducted on all earthquakes with a magnitude M>5 in the Antarctic waters, for latitudes less than 50. Earthquake data from a large number of sources were obtained, grouped, and analyzed. Based on the obtained data, a recurrence law for the Antarctic region was established.

## 5. References

Russia in Colors. Discovery of Antarctica: Fabian Bellingshausen and Mikhail Lazarev 2004-2015 [online] Available at http://ricolor.org/history/eng/expedition/antarctida/ [Accessed: 10 June 2025].

Bellingshausen, F.F. (1949), Double Explorations in the Southern Icy Ocean, M.: GIZ, 410 p.

Antarctic Stations [Electronic resource]: Wikipedia. The Free Encyclopedia. 2023. URL: https://ru.wikipedia.org/wiki/Антарктические_станции [Accessed: 10 June 2025]

Reading A. M. (2007). The seismicity of the Antarctic plate, *The Geological Society of America*, Canberra, ACT 0200, Australia, 285-298

The U.S. Geological Survey 1879. URL: https://earthquake.usgs.gov/earthquakes/search/.

International Seismological Centre 1964. URL: https://www.isc.ac.uk/.

SCALING LAWS // NOAA NCTR. URL: https://nctr.pmel.noaa.gov/education/ITTI/usgs/GPSthailand/lecture5.pdf.

Dubinin M. (2006), Calculating the distance and initial azimuth between two points on the sphere // GIS-LAB. [Electronic resource] // URL: https://gis-lab.info/qa/great-circles.html

Utsu, T. (1961). A Statistical Study on the Occurrence of Aftershocks. *The Geophysical Magazine*, 30, 521-605.

Ivchenko G.I., U.I.Medvedev (1984). Mathematical Statistics,Moscow: Higher School, p. 248 c.

Mazova R. Kh., E.N. Pelinovsky E., S.L.Solovyov (1983). Statistical data on the character of tsunami wave runup on the beach, *Okeanologe*, V.XX111, N.6, p.932-937.

Lobkovsky L., Mazova R., Tyuntyaev S., Remizov I (2016). Features and problems with historical great earthquakes and tsunamis in the mediterranean sea, , *Science of Tsunami Hazards*,. 35(3), 167-188